

Three-nucleon short range correlations studies in inclusive scattering for $0.8 < Q^2 < 2.8$ (GeV/c)²

J. Arrington (co-spokesperson), P. Solvignon (co-spokesperson), D. F. Geesaman,
K. Hafidi, R. Holt, P. Reimer

Argonne National Laboratory, Argonne, IL 60439

D. Higinbotham (co-spokesperson), D. Meekins

Thomas Jefferson National Accelerator Facility, Newport News, VA 23606

D. B. Day (co-spokesperson)

University of Virginia, Charlottesville, VA, 22901

Abstract

We propose to perform a precision test of scaling in the region dominated by scattering from three-nucleon short range correlations (3N-SRC) in Hall A. If scaling in this region is valid, then one can use the ratio of scattering from heavier nuclei to ³He as a measure of the relative contribution of 3N-SRC in heavier nuclei. The kinematics are chosen to emphasize the $x > 2.2$ region using an incident beam energy of 3.6 GeV, and the Hall A high resolution spectrometers in their standard configurations at several scattering angles from 15° to 29°. In addition to confirming the dominance of 3N-SRC, this measurement will be able to provide a better quantitative extraction of the contribution of 3N-SRC in nuclei, as well as providing more detailed information on the x and Q^2 dependence. Five nuclear targets will be used, ²H, ³He, ¹²C, ⁴⁰Ca and ⁴⁸Ca. By using calcium isotopes, we can have a first look at the isospin dependence of 2N- and 3N-SRC. The proposed experiment requires 11 days of beam time, including calibration, overhead, and background measurements, and uses only standard targets and detector configurations.

I. MOTIVATIONS

While the structure of nuclei is relatively well described in terms of the nuclear shell model, measurements of the spectroscopic factors in (e,e'p) and other transfer reactions show a significant missing strength, on the scale of 30–40% of the nucleons. Short range correlations (SRCs) provide the largest depletion of shell model strength. The short range repulsive core of the N–N interaction yields a significant probability of a hard interaction between nucleons in the dense medium of a heavy nucleus. This leads to a dramatic increase in the number of extremely high-momentum nucleons ($k > k_F$) in the nucleus.

While single nucleon knockout reactions allow us to look at the shell model contributions, it is much more difficult to probe the high-momentum nucleons generated by correlations, as the cross section in this region has extremely large contributions from other processes such as final-state interactions and meson-exchange currents. Inclusive electron scattering can be used to probe these high-momentum nucleons, providing cleaner measurements that complement the more detailed measurements possible in coincidence reactions.

Scattering from a proton is kinematically limited to values of Bjorken- x at or below one, with elastic scattering at $x = 1$. For a nucleus, $x \leq M_A/M_p \approx A$, but quasielastic scattering from a single nucleon occurs mainly for $x \approx 1$. The motion of the nucleon in the nucleus broadens the quasielastic (QE) peak, but for momenta at or below the Fermi momenta, k_F , there is little strength from QE scattering above $x = 1.2$ – 1.3 . Above this region, the cross section is dominated by scattering from the high-momentum nucleons generated by short range correlations. If we assume that the two-nucleon SRC involve only the two interacting nucleons and neglect their motion in the nucleus and any isospin dependence, the distribution of high-momentum nucleons coming from 2N-SRCs should be identical in all nuclei, and thus the high-momentum tail in a heavy nucleus should look similar to the high-momentum tail in deuterium, scaled up by the number of 2N-SRCs. This is the dominant contribution to the scattering up to $x = 2$, as the probability to have a multi-nucleon configuration generating high momentum nucleons is much smaller than the probability to have a two-nucleon configuration. However, for $x > 2$, the contribution from a stationary 2N-SRC vanishes and the scattering should be dominated by contributions from 3N-SRCs.

The main effect of the small motion of the correlation in the nucleus allows strength from a j -nucleon correlation to contribute to the scattering for values of x slightly larger than $j - 1$. Because of this, 2N-SRCs dominate for $1.3 \lesssim x < 2$ rather than for $1 < x < 2$, 3N-SRC dominate for $2.3 \lesssim x < 3$, and so on. We will return to the isospin dependence later.

Using this basic picture, Frankfurt and Strikman [1, 2] showed that the cross section for $x \gtrsim 1.3$ is a sum of contributions from 2N, 3N,... correlations,

$$\begin{aligned} \sigma_A(x, Q^2) &= \sum_{j=2}^A \frac{A}{j} a_j(A) \sigma_j(x, Q^2) \\ &= \frac{A}{2} a_2(A) \sigma_2(x, Q^2) + \frac{A}{3} a_3(A) \sigma_3(x, Q^2) + \dots, \end{aligned}$$

where σ_j is the cross section for scattering from a j -nucleon correlation and the constants $a_j(A)$ are proportional to the probability of finding a nucleon in a j -nucleon correlation which should fall rapidly with j as nuclei are dilute. Taking $a_j(A) = 1$ for $A = j$, i.e. defining $a_j(A)$ to be probability of finding a 2N-SRC in nucleus A relative to deuterium, the cross section σ_j reduces to the cross section for scattering from a nucleus with $A=j$, e.g. for $A = 2$, $\sigma_{eD}(x, Q^2) = a_j(A) \sigma_j(x, Q^2)$ and $\sigma_j(x, Q^2) = 0$ for $x > j$.

In the region where 2N-SRCs dominate, they predict scaling of the cross section ratios:

$$(2/A) \sigma_A(x, Q^2) / \sigma_D(x, Q^2) = a_j(A) / a_j(D) = a_j(A) \quad (1)$$

where the factor $(2/A)$ yields the ratio of cross sections per nucleon. Thus, for all values of x and Q^2 where the scattering is dominated by 2N-SRCs, the ratio of the cross section from a heavy nucleus to deuterium (or in fact the ratio of any two nuclei) should be independent of x and Q^2 , and be a direct measure of the relative number of 2N-SRCs in the nuclei. While this neglects the effects of FSI, it has been argued [3] that in these small-sized SRCs,

only the FSI between the nucleons within the correlation matter, and that these FSI should be identical as long as the nature of the correlations is identical for all nuclei, as assumed in the SRC model.

This scaling behavior for 2N-SRCs was first observed in SLAC data [2, 4], and more recently in Hall C and Hall B at Jefferson Lab [5, 6]. The newest results from CLAS provided the first direct evidence for such scaling in the 3N-SRC region, as shown in Figure 1.

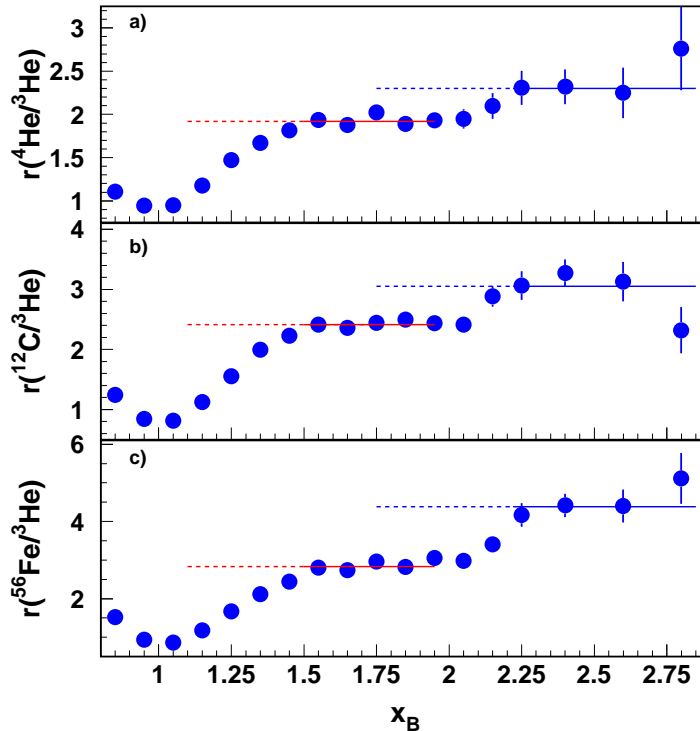


FIG. 1: 2N and 3N correlations from recent JLab Hall B data [6]. See text for definition of r .

Because these are ratios to ${}^3\text{He}$, which is not an isoscalar nucleus, a correction has to be applied for the difference between σ_p and σ_n . Thus, the ratio plotted is not the cross section ratio, $R(A, 3He) = \sigma_A/\sigma_{3He}$, but instead is taken to be

$$r(A, {}^3\text{He}) = K_3(\sigma_n, \sigma_p)R(A, {}^3\text{He}) \quad (2)$$

with $K_3(\sigma_n, \sigma_p) = A(2\sigma_p + \sigma_n)/3(Z\sigma_p + N\sigma_n)$ and was found [6] equal to 1.14 ± 0.02 for ${}^4\text{He}$ and ${}^{12}\text{C}$, and 1.18 ± 0.02 for ${}^{56}\text{Fe}$ for the kinematic range of this measurement. The data is shown for Q^2 between 1.4 and $2.6(\text{GeV}/c)^2$ (with an average Q^2 value of $1.5\text{--}1.6(\text{GeV}/c)^2$). For $x > 1.5$, the 2N-SRC dominated region, there is high statistics data over a large range in Q^2 , and it was observed [5, 6] that for $Q^2 > 1.4$, scaling in the 2N-SRC region was valid for $1.5 < x < 2$. For the 3N-SRC region, the cross section is much smaller, and all data for $Q^2 > 1.4$ were combined, yielding signs of a plateau in x , which suggests that the data are in the scaling region.

This was the first direct indication of scaling in the x -region between 2.25 and 2.80, corresponding to dominance of three-nucleon short range correlations. But these data are have significant limitations that make it difficult to make a quantitative extraction of the 3N-SRC probabilities, or even to ensure that the measurement is directly sensitive to the 3N-SRC contributions.

II. SUMMARY OF PREVIOUS MEASUREMENTS

There have been several measurements of in the 2N-SRC region, providing sufficient data to measure the relative 2N contributions in light and heavy nuclei, test the x and Q^2 dependence to verify scaling. While the only published results showing ratios of few-body and heavy nuclei to deuterium come from combining different measurements, Hall C experiments E89-008 and E02-019 made direct measurements of few-body and heavy nuclei to deuterium, and measured absolute cross sections in addition to ratios to help provide further tests of scaling and FSI contributions at large x . So while there are limitations with each of these previous extractions in the 2N-SRC region, the combined results from these measurements should give a relatively complete picture of most of the issues for 2N-SRCs. The main outstanding issue is the isospin dependence, discussed in Sec. III, where we can provide some new information in inclusive scattering to complement the two-nucleon knockout data from Hall A experiment E01-015 [7, 8].

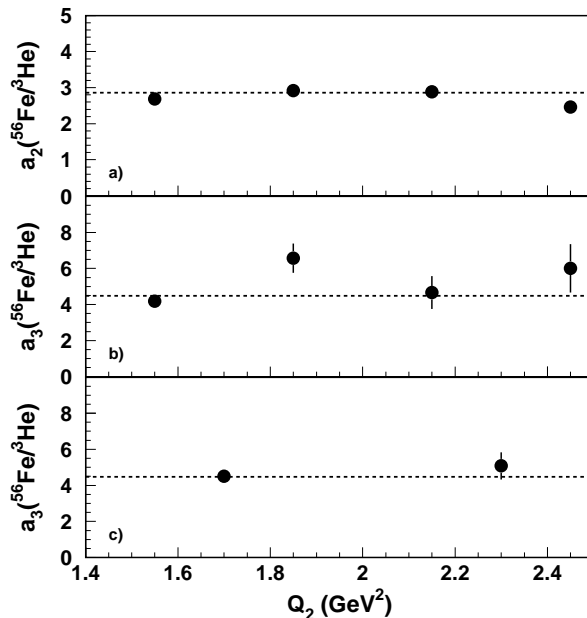


FIG. 2: Q^2 -dependence of 2N and 3N correlations for ^{56}Fe from recent JLab Hall B data [9]. See text for definition of $a_3(^{56}\text{Fe}/^3\text{He})$.

The recent CLAS data [6] provide the best measurement of 3N-SRCs, but there are limitations in the data. First, there was not enough data to look at the Q^2 dependence of the ratios, as most of the statistics are in the lowest Q^2 bin. Figure 2 shows the average values of a_2 (top) and a_3 (middle) extracted from the ratio of $\text{Fe}/^3\text{He}$ for four Q^2 bins. For a_2 , we can see that the ratio is essentially Q^2 independent above 1.4 GeV^2 , and also that the ratio is x -independent for each of these Q^2 bins [5]. For a_3 , the average value is only precisely measured for the lowest Q^2 , and in fact the lowest Q^2 bin is $\sim 30\%$ below the average of the higher Q^2 bins, and differs by about 2.5σ . The statistics are such that there is no real verification of the Q^2 -independence of the ratio, and even when combining all data above $Q^2 = 1.4 \text{ GeV}^2$, the data is consistent with being independent of x above $x = 2.25$ (Fig. 1, but the data do not allow us to set strong limits on the x dependence in this region. In addition, the moderate resolution of the CLAS detector leads to a smearing in the observed x -dependence. While this should cancel in the target ratios, it makes it more difficult to quantify the cutoff in x where the correlations dominate.

The experiment assumed that scaling set in for 3N-SRC at the same Q^2 as for 2N-SRC, and then averaged the data above $x = 2.25$. If one wants to isolate 3N-SRCs by probing above some minimum nucleon momentum, then for a reasonably large Q^2 value, there is an x value above which one probes above that minimum nucleon momentum [5],

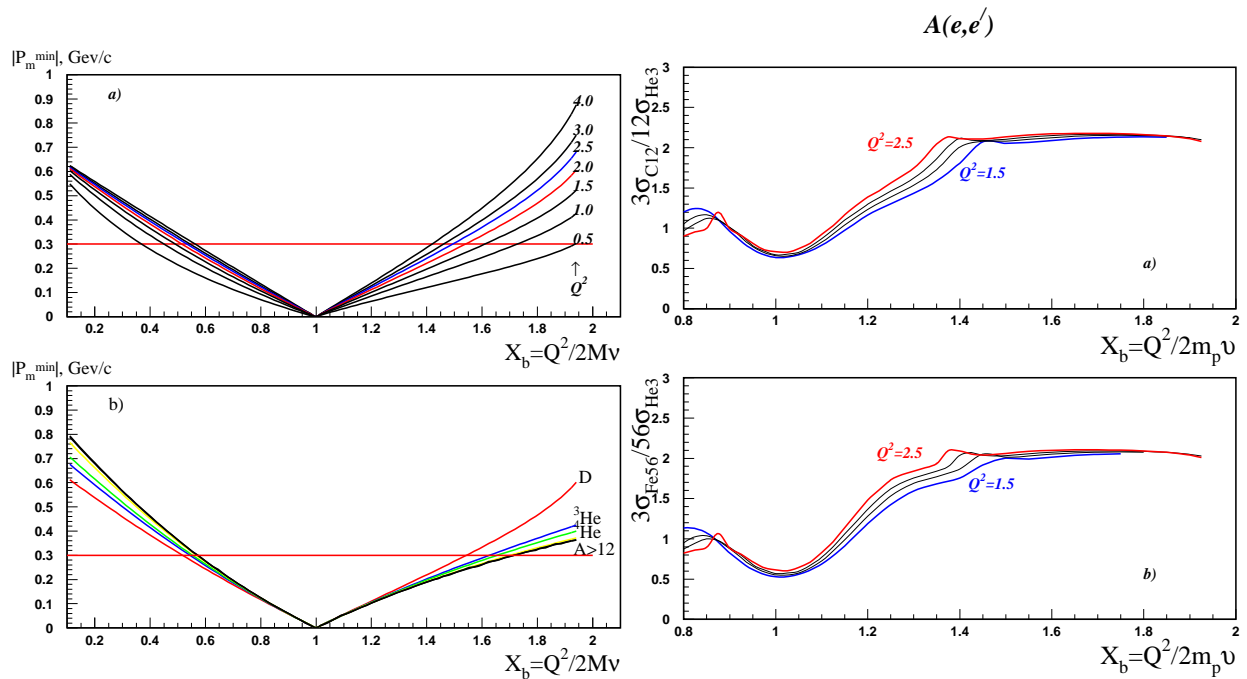


FIG. 3: Left: Minimum nucleon momentum probed as a function of x and Q^2 for deuterium (top) and as a function of x and A for $Q^2 = 2.0$ GeV² (bottom). Right: Plot showing calculated $A/{}^3\text{He}$ ratio for four Q^2 values, showing the Q^2 dependence of the scaling region in x (from [10]).

as one sees in Fig. 3. Given that we cannot study scaling as a function of Q^2 for this data, or even make a strong quantitative statement about the region of x above which scaling is observed, it is difficult to make a quantitative extraction of $a_3(A)$. As observed in Fig. 2, the lowest Q^2 point dominates the averaging. Thus, the result may not be reliable if the scaling region has not yet been reached. For example, the average of the three last points gives approximately $a_3({}^{56}\text{Fe}/{}^3\text{He}) \approx 5.8 \pm 0.6$, compared to the lowest Q^2 point, which gives $a_3({}^{56}\text{Fe}/{}^3\text{He}) \approx 4.2 \pm 0.2$. So 80–90% of the statistics come from the lowest Q^2 bin, which is approximately 2.5σ from the average of the higher Q^2 data. This is not strong enough to conclude that scaling is *not* valid, but makes it difficult to argue that scaling has been demonstrated at the level necessary for a quantitative extraction of the 3N-SRC probabilities. More precise data, especially at somewhat larger Q^2 , are needed to precisely determine $a_3(A/{}^3\text{He})$ and to clarify its Q^2 and x dependence.

III. ISOSPIN EFFECTS ON SRC

Another question raised is the isospin dependence of short-range correlations. While the ratios shown above are corrected for the difference between the electron-proton and electron-neutron cross sections, they assume that the ratio of protons and neutrons in the 2N-SRCs and 3N-SRCs is equal to the N/Z ratio of the nucleus. This is true if one assumes that the nature of the correlations is independent of the isospin. For 2N-SRCs, a global analysis [11] of the inclusive data discussed above and $A(p,ppn)$ reactions [12, 13] as well as new results from ${}^{12}\text{C}(e,e'pN)$ measurements in Hall A [8, 14] suggest that 90% of the 2N-SRCs in ${}^{12}\text{C}$ are pn , while the nn and pp correlations provide only around 10% of the 2N-SRCs. Recent calculations [15] show that for 2N-SRCs at rest in a nucleus, the Tensor force yields an excess of high-momentum nucleons in deuteron-like ($T=0$) np correlations, while nn , pp , and $T=1$ np pairs are all strongly suppressed.

We can study these effects using inclusive scattering in the 2N-SRC (or 3N-SRC) dominated regions for nuclei with different N/Z ratios. While detailed calculations exist for few-body nuclei, it is easy to see the impact of these for a

simple case; the comparison of ${}^3\text{He}$ and ${}^3\text{H}$. For isospin-independent 2N-SRCs, ${}^3\text{He}$ will have two pn pairs and one pp pair, compared to two pn pairs and one nn pair for ${}^3\text{H}$. For ${}^3\text{He}$, this yields four options for a high-momentum proton and two for a high-momentum neutron, yielding a proton distribution that is twice the neutron distribution at large momenta. For ${}^3\text{H}$, the opposite happens, but in both cases, the ratio of the proton to neutron momentum distributions, $n_p(k)/n_n(k)$ at high momentum is just equal to the Z/N ratio for the proton. If deuteron-like SRCs dominate, then each nucleus has two possible pn pairs and negligible contributions from pp or nn pairs, yielding $n_p(k)/n_n(k) = 1$ for $k > k_F$.

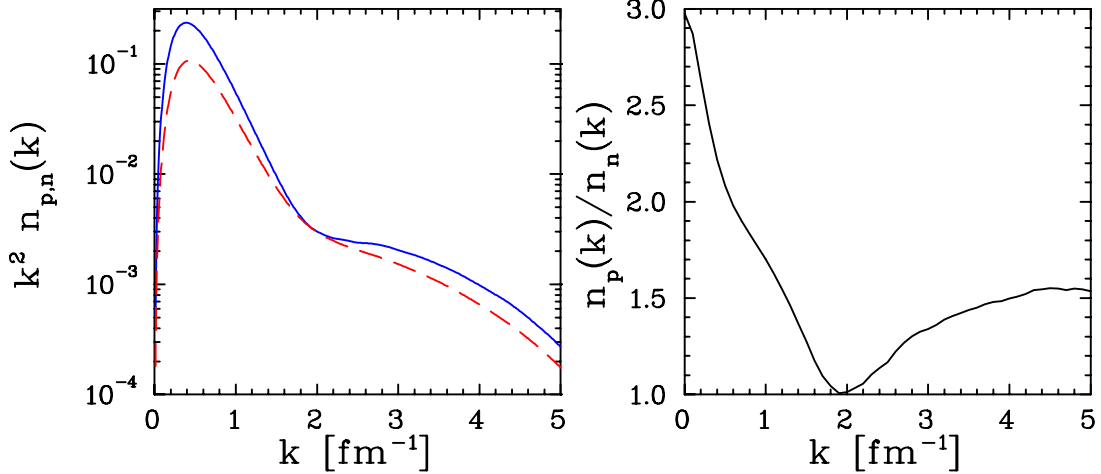


FIG. 4: Left: Momentum distribution for protons (solid) and neutrons (dashed) in ${}^3\text{He}$ from Quantum Monte Carlo calculation [16, 17]. Right: Ratio of proton to neutron distributions.

Figure 4 shows the momentum distribution for protons and neutrons in ${}^3\text{He}$, as well as the ratio. For this calculation, the ratio at high momenta, where 2N-SRCs dominate, is approximately 1.5 at the largest moment (with a weighted average closer to 1.2 for $k > k_F$). Other calculations yield somewhat different results (*1.7 according to my memory of Strikman's statement about Sargisan's calculation*). Similar issues will of course arise in the region of 3N-SRC dominance.

Such measurements with ${}^3\text{H}$ and ${}^3\text{He}$ will be possible using the moderate-density ${}^3\text{H}$ target proposed for E12-06-118 [18]. Because of the lower density of the target, it will be important to know what Q^2 is required to reliably access the scaling region for both 2N and 3N-SRCs, making the measurements proposed here valuable for designing such an experiment, as well as optimizing the approved measurement E12-06-105 which will make measurements at $x > 2.5$ for a variety of few-body and heavy nuclei. In the meantime, we can make similar measurements using heavier nuclei (${}^{40}\text{Ca}$ and ${}^{48}\text{Ca}$), which also cover a large range in the ratio of N/Z.

For the kinematics of this measurement, the cross section for scattering from a proton is approximately three times the cross section for scattering from a neutron. If the ratio of protons to neutrons goes like N/Z at large momenta, then the cross section per nucleon should be approximately 8% lower for ${}^{48}\text{Ca}$, due to the 40% increase in the number of neutrons:

$$\frac{\sigma(e^{48}\text{Ca})/48}{\sigma(e^{40}\text{Ca})/40} = \frac{(20\sigma_p + 28\sigma_n)/48}{(20\sigma_p + 20\sigma_n)/40} \approx \frac{(20\sigma_p + 28\sigma_p/3)/48}{(20\sigma_p + 20\sigma_p/3)/40} = 0.916 \quad (3)$$

If we take the extreme case, where only np correlations matter for large x , then there are 20² possible np pairs in ${}^{40}\text{Ca}$ and 20*28 in ${}^{48}\text{Ca}$. Scaling to the number of nucleons, this gives

$$\frac{\sigma(e^{48}\text{Ca})/48}{\sigma(e^{40}\text{Ca})/40} = \frac{(20 * 28)/48}{(20 * 20)/40} = 1.17 \quad (4)$$

or a 17% increase in the cross section per nucleon for ${}^{48}\text{Ca}$, compared to the isospin-independent expectation of an 8.4% decrease. This assumes that any pair of nucleons can be part of a correlated pair, while the fact that the

ratio of $A/{}^2\text{H}$ saturates at a value of 5–6 implies that only a certain number of “nearest neighbors” are involved in forming SRCs. However, the ratio of neutrons to protons that can participate scale with the total number of neutrons and protons, yielding essentially the same results if we limit ourselves to a subset of nearest neighbors in determining these ratios. There will also be a small correction due to the difference in the ratio of surface to volume between ${}^{40}\text{Ca}$ and ${}^{48}\text{Ca}$. Because the number of 2N-SRCs depends only weakly with A for heavier nuclei (Ref. [4] extracts $a_2({}^{12}\text{C})=5.0\pm 0.5$, $a_2({}^{197}\text{Au})=4.8\pm 0.7$, the correction due to the mass difference between ${}^{40}\text{Ca}$ and ${}^{48}\text{Ca}$ will be negligible compared to the 25% difference between the expectation for isospin-independent and pn-pair dominance pictures.

Recently theoretical efforts have been put into the expression of the equation of state for asymmetric nuclear matter [19] which is essential in the understanding of the neutron stars. One of the challenging feature of this theoretical work is to address the nucleon-nucleon interaction behavior in symmetric nuclear matter and in pure neutron matter. In their approach, they predict a significant discrepancy between the neutron and proton momentum distributions for an asymmetric factor $(N-Z)/A$ of 0.2, corresponding to ${}^{48}\text{Ca}$. This calculation is in good agreement with previous experimental results showing that protons are more affected by correlations due to interactions with out-numbered neutrons.

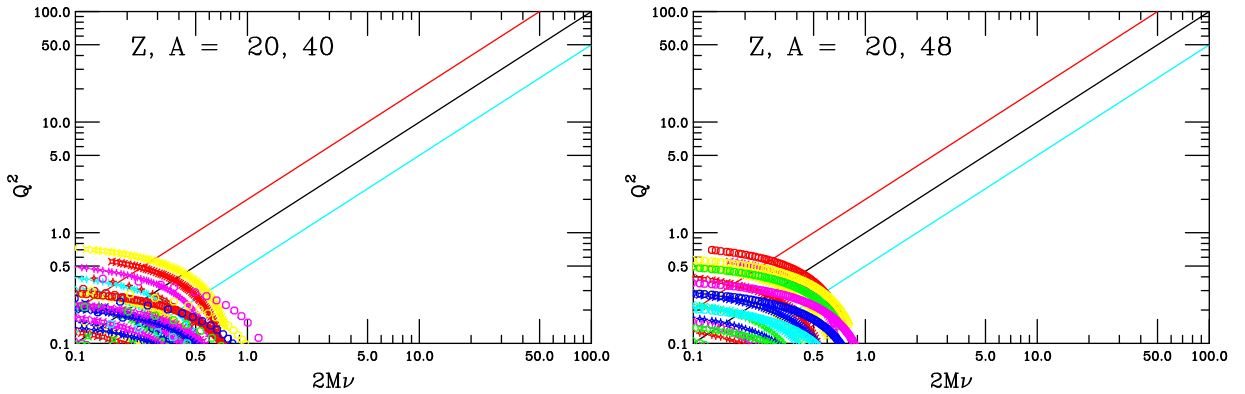


FIG. 5: Kinematic coverage of existing ${}^{40}\text{Ca}$ and ${}^{48}\text{Ca}$ data as a function of Q^2 and $2M\nu$. The middle (black) line shows $x=1$, while the top (red) line shows $x=2$.

Figure 5 shows the kinematic coverage of existing data on ${}^{40,48}\text{Ca}$. While the data on ${}^3\text{He}$ and the $A/{}^3\text{He}$ will provide significant improvements over previous existing data, the data on ${}^{40,48}\text{Ca}$ is entirely limited to lower Q^2 , and no such measurements of the isotopic dependence of the correlations exist for medium or heavy nuclei. The only data looking at the isotopic dependence of SRCs is the comparison of ${}^3\text{He}$ and ${}^4\text{He}$ in the CLAS data and the E02-019 results which, as stated earlier, are limited in their precision and, for the CLAS data, their kinematic coverage. Another advantage of the comparison of ${}^{40}\text{Ca}$ and ${}^{48}\text{Ca}$ is the fact that the A dependence of the SRC probability appears to be extremely weak for medium and heavy nuclei, while it is significant for $A<12$. Finally, the A -dependence of the minimum momentum probed for a given x and Q^2 setting is strong for light nuclei, but weak for heavier nuclei (Left plot, bottom panel of Fig. 3). Thus, it is more critical for the comparison of few-body nuclei that the scaling region has been reached.

IV. THE PROPOSED MEASUREMENT

We propose to perform precision measurements of the inclusive electron scattering cross sections for ${}^2\text{H}$, ${}^3\text{He}$, ${}^{12}\text{C}$, ${}^{40}\text{Ca}$ and ${}^{48}\text{Ca}$ with an incident beam energy of 3.6 GeV and at eight scattering angles: 15° , 17° , 19° , 21° , 23° , 25° , 27° and 29° . Our focus is on the $x > 2$ region; Fig 6 shows the x and Q^2 coverage of the proposed experiment.

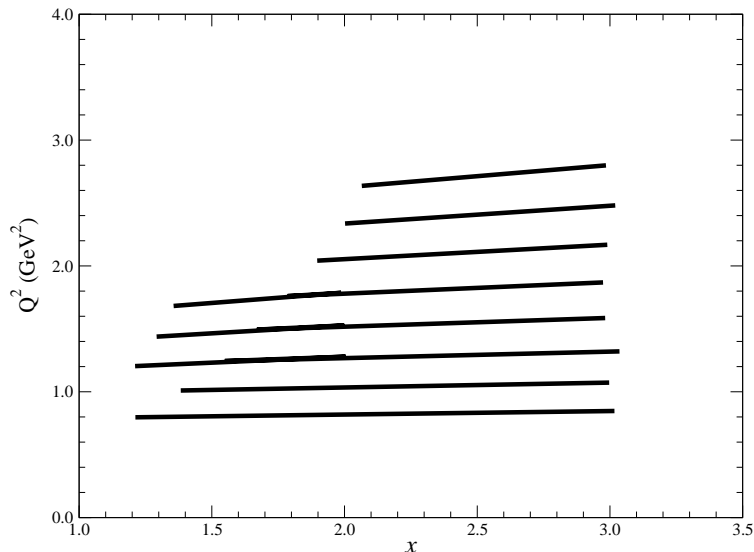


FIG. 6: Proposed kinematic coverage. Note that this shows only the central $\pm 3\%$ of the HRS momentum acceptance, but the acceptance is relatively uniform out to $\pm 4.5\%$

A. Background

Cryotarget: Aluminum window contribution

The ^2H and ^3He cryotargets are contained in 20cm aluminum cans made from Aluminum 7075-T6 of density of about 2.8g/cm^3 . The aluminum windows are equivalent to $\approx 13\%$ of the ^3He thicknesses (Table I). Because the ratio of the Al to ^3He cross sections in the 3N-SRC region is roughly 3–4 (based on Fig. 1), the Al contribution is approximately 45% of the ^3He cross section on the ^3He target, so contributes $\approx 35\%$ of the total cross section. Fig. 7 illustrates the contamination of the aluminum window in a 4cm ^3He cell. In the region of interest of our proposed measurement ($x \gtrsim 2.3$), the endcap contributes more than half of the total cross section. By using a 20cm cell, we should be able to reduce this contribution by at least a factor 5. Moreover, the resolution of the two HRS allows us to perform a software cut to remove the endcap contributions. We also plan to take data on an empty aluminum can with the same thicknesses to test the efficiency of the cuts, and to subtract any residual endcap contribution. We can also test this by removing the software cuts and subtracting the full endcap contribution.

Target	$T(\text{K}), P(\text{psia}), L(\text{cm})$	Thickness(g/cm^2)
^2H	22.0, 22.0, 20.0	3.35
^3He	8.0, 200.0, 20.0	1.38
Al Entrance	N/A, N/A, 0.035	0.09
Al Exit	N/A, N/A, 0.035	0.09
Al Wall	N/A, N/A, 0.035	0.09

TABLE I: Aluminum window/wall thickness and running conditions of the cryo-target (from [20])

Pion contamination and charge-symmetric background

The expected pion background has been evaluated using experimental data of JLab Experiment E89-008 [22]. For an incident energy of 4.045GeV and at a scattering angle of 23° , the π/e ratio was found to be approximately 10:1 for a 2% RL carbon target at a momentum setting of 3.76GeV and 4:1 for a 2% RL iron target at 3.60GeV.

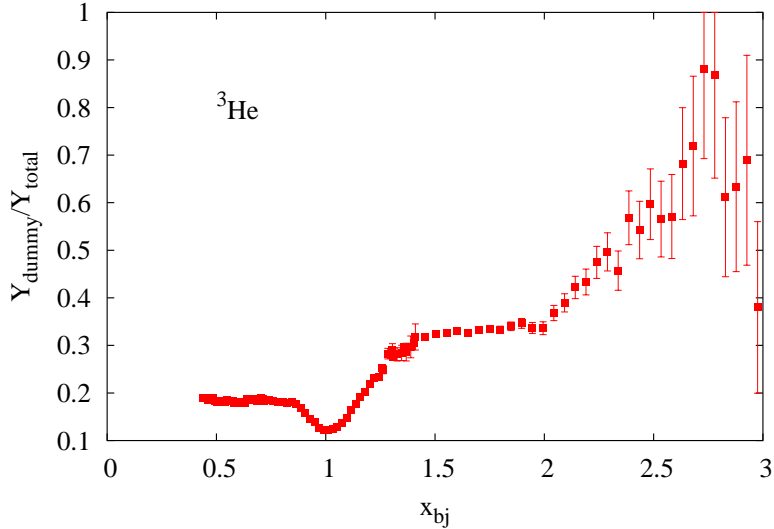


FIG. 7: Dummy contamination from JLab Experiment E02-019 data for a 4cm cell. Plot from Ref. [21].

The PID performance of Hall A HRS detectors has been shown to be very good in past experiments (see [23, 24], for example) allowing a reduction of the pion background by a factor of about 10^4 , while keeping an electron efficiency better than 99%, when CO_2 gas Čerenkov counter and double-layer lead glass calorimeter are associated. This yields a worst-case pion contamination of $\approx 0.1\%$.

The charge-symmetric background can be very large for large scattering angles, but decreases rapidly at smaller angles. For E02-019 [21], the charge-symmetric background for even the high-Z, 6% radiation length targets was always well below 1% for angles below 30° and relatively large values of x ($x \gtrsim 0.6$). For the targets proposed here and scattering angles below 25° , we expect a maximum charge-symmetric background to be below 0.1%.

B. Projected results

To estimate the coverage and the precision of the proposed measurements, a conservative momentum bite of $\pm 3\%$ was used. This is sufficient to fully cover the 3N-SRC region in one setting, although using the full HRS momentum acceptance will improve the coverage in the 2N-SRC region. The data were binned in x with a binsize of 0.1. Respecting the beam current allowed on each target (see Table II) and data acquisition limit ($=4\text{kHz}$), the projected statistical uncertainties were estimated after optimizing the limited time available for the measurements. For the cryotarget, the beam current limitation is due to the coolant restriction.

Target	T (K)	P (psia)	length (cm)	RL (g/cm^2)	I^{limit} (μA)
^2H	22.0	22.0	20.0	3.35	60.0
^3He	8.0	200.0	20.0	1.38	60.0
	thickness (cm)				
^{12}C		0.50		0.95	80.0
^{40}Ca		0.65		0.99	40.0
^{48}Ca		0.65		0.99	40.0

TABLE II: Cryo-target characteristics from [20] (top part) and, solid targets and their characteristics asked for this proposal (bottom part).

The rates for ${}^3\text{He}$ were evaluated using the XEM cross section model [21] based on y-scaling for the large x region. The XEM model was fitted to data on a variety of light and heavy nuclear targets for both the DIS and $x > 1$ region, but with a beam energy of 5.8 GeV. Figure 8 shows a comparison of the model compared with existing data for ${}^3\text{He}$ [25] at lower Q^2 , closer to the range of the proposed measurements. At these lower Q^2 values, the model is still in good agreement with the data from SLAC [26]. While the model is fit to the E02-109 kinematics (3-4 GeV 2), it is good at approximately the 20% level down to Q^2 values below 0.5 GeV 2 based on a comparison to the database [25] and also at higher Q^2 values between 1.0 and 4.0 GeV 2 [23].

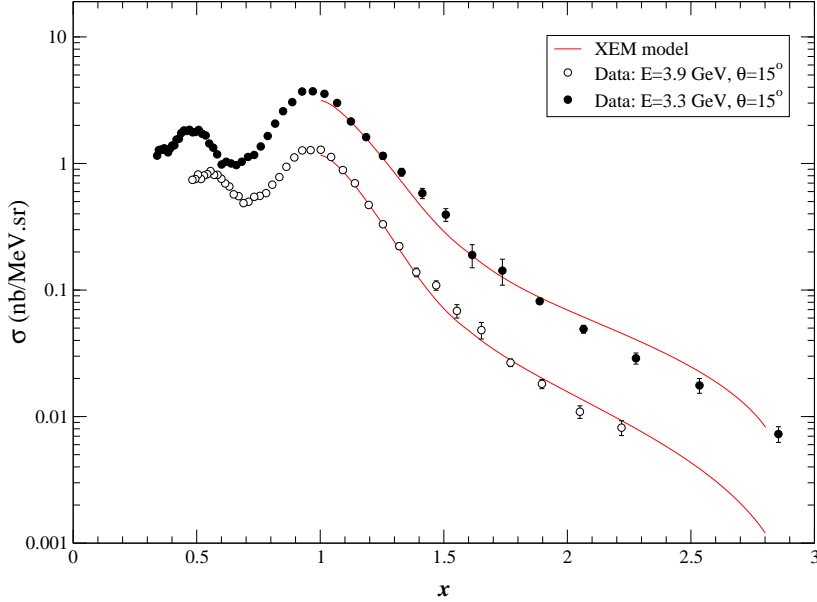


FIG. 8: Comparison of the XEM cross section model with world data from [25].

The cross sections for heavier nuclei (carbon and calcium isotopes) were estimated using the XEM model for ${}^3\text{He}$ and the ratio $A/{}^3\text{He}$ from the Hall B SRC results. Considering that the scaling factor between the model and Hall B at a given x for the nucleus $A > 3$ is S_A , we can write:

$$S_A \cdot r_{A/{}^3\text{He}}^{model} = r_{A/{}^3\text{He}}^{HallB} \Rightarrow S_A \cdot \sigma_{A>3}^{model} = \sigma_{A>3}^{HallB} \quad (5)$$

The resulting uncertainty on the ratio from the scaled model will be expressed as follows:

$$\Delta r_{A/{}^3\text{He}} = r_{A/{}^3\text{He}}^{HallB} * \sqrt{\left(\frac{\Delta \sigma_A^{model}}{\sqrt{S_A} \cdot \sigma_A^{model}}\right)^2 + \left(\frac{\Delta \sigma_{{}^3\text{He}}^{model}}{\sigma_{{}^3\text{He}}^{model}}\right)^2} \quad (6)$$

For calcium isotopes, a logarithmic extrapolation with respect to A was done to estimate the values of $a_2({}^{40,48}\text{Ca}/{}^3\text{He})$ and $a_3({}^{40,48}\text{Ca}/{}^3\text{He})$. Then the ${}^{40,48}\text{Ca}$ cross sections from the model were scaled using the same procedure as above. These estimates do not account for any isotopic dependence in the cross section, and so yield essentially identical values for ${}^{40}\text{Ca}$ and ${}^{48}\text{Ca}$, rather than the 25% difference one would expect if np correlations dominate and one follows the same approach as in the past, i.e. applying the naive correction for the neutron excess based on the N/Z ratio.

The ${}^2\text{H}$, carbon and calcium isotopes target running times were optimized by requiring that the contribution of the relative uncertainty from nucleus A is equal to the ${}^3\text{He}$ one in Eq (6), or:

$$\frac{\Delta \sigma_A}{\sqrt{S_A} \cdot \sigma_A} = \frac{\Delta \sigma_{{}^3\text{He}}}{\sigma_{{}^3\text{He}}} \quad (7)$$

θ	E'	x_{range}	Q_{range}^2	time (hrs)		
deg	(GeV)		(GeV ² /c)	¹² C+ ⁴⁰ Ca+ ⁴⁸ Ca	³ He	² H
15.0	3.350	1.2-3.0	0.80-0.85	1.8	2.0	2.7
17.0	3.310	1.4-3.0	1.01-1.07	2.5	2.4	1.7
19.0	3.165	1.2-2.0	1.20-1.28	2.5	2.4	2.5
19.0	3.270	1.6-3.0	1.24-1.32	5.1	3.0	2.1
21.0	3.220	1.7-3.0	1.49-1.59	10.2	6.0	4.2
23.0	3.170	1.8-3.0	1.76-1.87	20.5	12.0	-
25.0	3.120	1.9-3.0	2.04-2.17	40.9	24.0	-
29.0	3.010	2.1-3.0	2.64-2.80	41.0	24.0	-
Total time needed (LEFT)				124.5	75.8	13.2
21.0	3.100	1.3-2.0	1.44-1.53	5.1	3.0	2.1
23.0	3.030	1.4-2.0	1.68-1.79	10.2	6.0	4.2
27.0	3.070	2.0-3.0	2.34-2.48	71.6	42.0	-
29.0	3.010	2.1-3.0	2.64-2.80	41.0	24.0	-
Total time needed (RIGHT)				127.9	75.0	6.3

TABLE III: Estimated beam time needed for the proposed experiment.

The angular acceptance $\Delta\Omega$ was estimated at 3.2msr and a conservative momentum bite ΔP of $\pm 3\%$ was chosen. The estimate time needed at each of the eight kinematic settings is given Table III.

The projected statistical uncertainties from the run times listed in Table III (assuming 100% efficiency) are plotted in Fig. 9. In Fig. 10, we show the uncertainties and Q^2 -coverage we can achieve in the study of the Q^2 -dependence of $a_3(A/{}^3\text{He})$. Also we show $a_2(A/{}^3\text{He})$, even if it is not the primary goal of the proposed experiment, and we will plan to obtain the same precision for $a_2(A/{}^2\text{H})$. We also plotted in Fig. 9 the projected statistical uncertainties for the ratios ${}^{40}\text{Ca}/{}^{12}\text{C}$, ${}^{48}\text{Ca}/{}^{12}\text{C}$ and ${}^{48}\text{Ca}/{}^{40}\text{Ca}$ which will be of great interest in the understanding of the isospin dependence of the short-range correlations.

The CLAS measurements had statistical uncertainties of $\approx 5\%$ and experimental systematic uncertainties of $\approx 7\%$. This does not include corrections for Coulomb distortion, estimated to be $\approx 5\%$ for the data on Iron. It also assumes that $Q^2 > 1.4 \text{ GeV}^2$ and $x > 2.25$ is sufficient to be in the scaling region, although the result for Iron would change by more than 30% and the statistical uncertainties grow significantly if a cut of $Q^2 > 1.7 \text{ GeV}^2$ were applied (Fig. 2).

If we ignore the issue of validity of the scaling assumption, the uncertainty on the experimental ratio of cross sections is $\approx 10\%$. There are greater systematic uncertainties in their extraction of the SRC probability from the experimental yield ratios. The combination of Coulomb corrections and SRC-motion, which were estimated but *not* applied, along with the experimental systematics due to combining data from different run periods, led to a total uncertainty of $\approx 25\%$. We will achieve much better statistics, allowing for a careful examination of the x and Q^2 dependence. Because we will take all of the data at one time, with no kinematic changes between targets, the experimental systematics on the measured cross section ratios will be at the 2-3% level or better. In extracting the relative strength of the 3N-SRC configurations, we will apply corrections for Coulomb distortion and center-of-mass motion of the SRC, which will yield *total* uncertainties on the ratio of 3N-SRC of $\sim 10\%$, dominated by the uncertainty in these corrections. Thus, both the direct experimental measurement and the extracted information on 3N-SRCs will be a factor of two or more better than the published CLAS results.

Finally, the CLAS measurement extracted only the normalized yield ratios, it did not measure the cross sections for the individual targets. Measurements of the absolute cross section for ${}^2\text{H}$ as $x \rightarrow 2$ and ${}^3\text{He}$ as $x \rightarrow 3$ will provide additional information that can be used to study the impact of final state interactions on the inclusive cross section in the 2N and 3N-SRC regions. While FSI are expected to be limited to interactions between the nucleons in the SRC, and thus cancel in the target ratios, this assumes that there is no isospin dependence in the FSI. Thus, comparisons to cross section calculations using realistic ${}^3\text{He}$ distributions will allow us to determine the size of FSI, or else to set

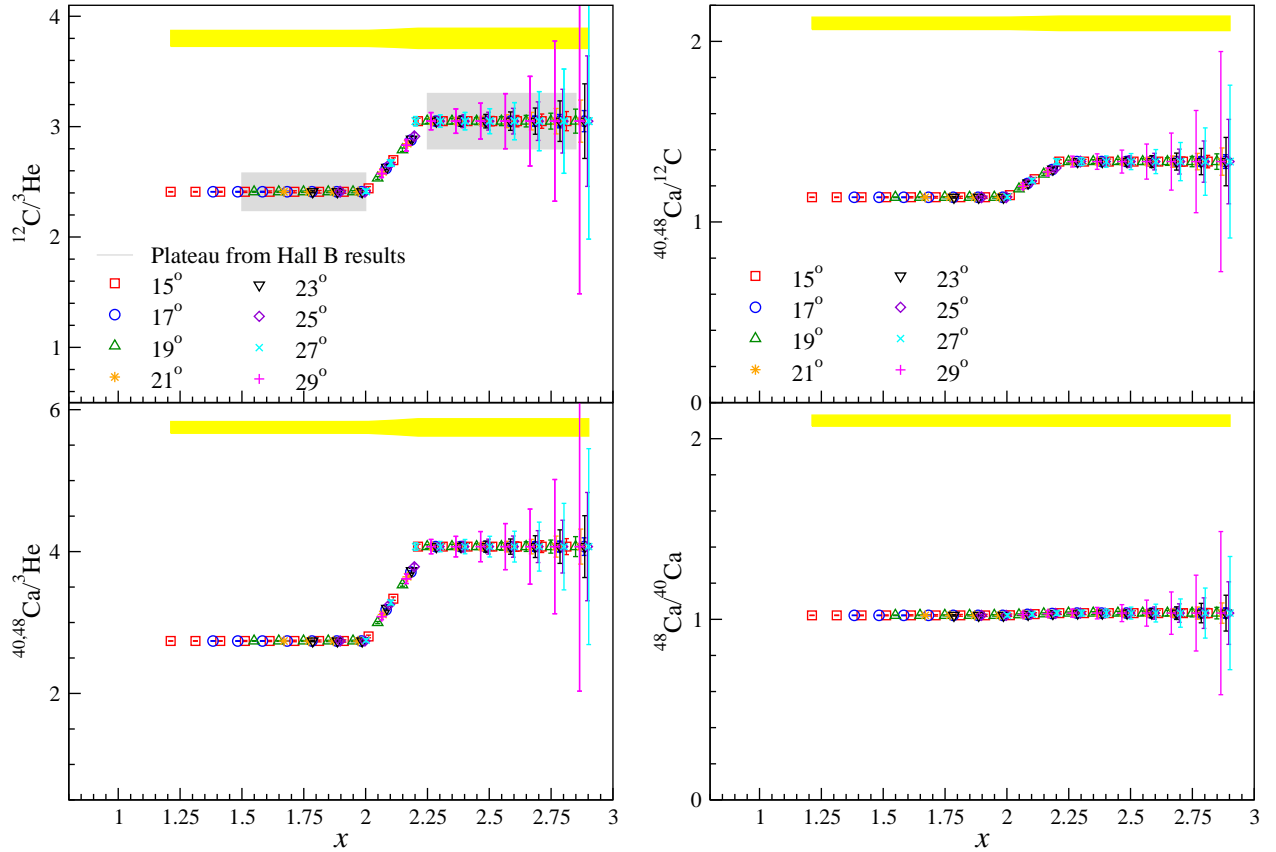


FIG. 9: Projected statistical uncertainties for data taken at a beam energy of 3.6 GeV and at the 8 scattering angles. The grey bands represent the resulting fits of the 2N and 3N correlations from recent JLab Hall B data [6]. The yellow bands represent a relative systematic uncertainty of 3%. Only the high x setting for 19, 21 and 23° have been plotted for clarity.

limits on the size of FSI. For ${}^2\text{H}$, a significant amount of data exist for moderate Q^2 and $x \rightarrow 2$, which allow us to map out the Q^2 dependence of these FSI, and which show that for larger Q^2 , there is no indication of significant FSI contributions, even between nucleons in the 2N-SRC. The proposed measurements will allow for improved studies of the analogous case for 3N-SRC in ${}^3\text{He}$, where we have a reliable baseline for the cross section in the absence of FSI.

Table IV summarizes the systematic uncertainties for this measurement.

C. Overhead time

The total overhead time needed for calibration, background study and configuration changes is now evaluated.

Calibration and background studies

We will need to measure the contributions from the aluminum entrance and exit windows of the cryo-target. For each kinematic, 20% of the ${}^3\text{He}$ running time should be enough to accomplish a precise dummy subtraction. Taking into account the parallel running of the left and right HRS, the time needed for dummy running is 16 hours.

A beam energy measurement (2 hrs) and BCM calibrations (2 hrs) will be necessary. We will take optics data at all scattering angles. A 30 minute run on carbon foils for each angle will be sufficient, for a total of 4 hours of optics

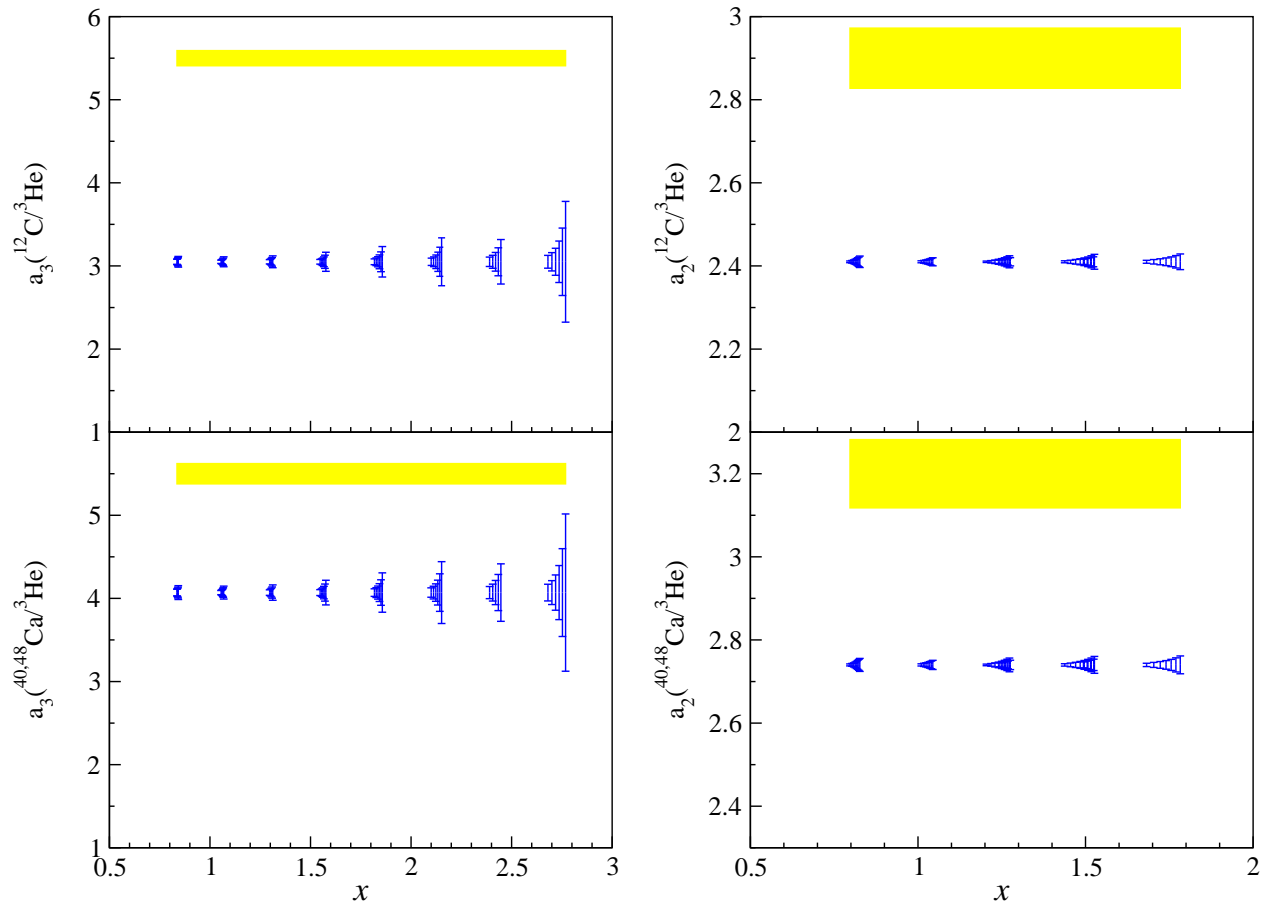


FIG. 10: Projected statistical uncertainties on the Q^2 -dependence of the 3N SRC (left plots) for all 8 scattering angles. The y-axis scale was chosen to match Fig. 2, which had average Q^2 of 1.4–1.5 (GeV/c) 2 . The 2N SRC projected statistical uncertainties are shown on the right plots. The yellow bands represent a conservative relative systematic uncertainty of 3%.

data. We assume 8 hours for initial checkout, yielding a total of 30 hours for setup, calibration, and background studies.

Configuration changes

Taking into account the fact that the left and the right HRS will be running in parallel, we require 8 hours for 8 kinematic changes (angle and HRS momentum), and 7.5 hours for 45 target changes, assuming 10 min. each. This yields a total of 15.5 hours for configuration changes.

V. REQUEST TO THE LABORATORY

We are requesting 265 hours (11 days) of beam time: 217 hours for the main data taking, 16 hours for configuration changes, and 32 hours for calibration, checkout, and background runs, all assuming 100% efficiency. We will need the 20cm ^2H and ^3He cryotargets, and empty cell, the multi-foil optics targets, and three solid targets: 2%RL-Carbon, 4%RL-Calcium-40 and 4%RL-Calcium-48 targets, to achieve our physics goal.

Systematic	$\delta\sigma/\sigma$	$\delta R/R$
Acceptance correction	2.0%*	2.0%
Radiative correction	3.0%*	0.3%
Tracking efficiency	1.0%*	-
Trigger efficiency	0.5%*	-
PID efficiency	1.5%*	-
Target density	0.5-2.0%	0.5-2.0%
Charge measurement	0.5%	0.5%
Energy measurement	0.05%	-
COMBINED UNCERTAINTY	4.1-4.6%	2.1-2.9%

TABLE IV: Relative systematic uncertainties in the extraction of the unpolarized cross sections from E01-012 [23] and of the cross section ratio from E03-103 [27]. Entries with an asterisk indicate corrections made directly on the cross section. Entries without asterisk indicate contributions to the overall uncertainty.

VI. SUMMARY

The proposed experiment will provide precise measurement on a_2 and a_3 for ^{12}C , ^{40}Ca , ^{48}Ca . The calcium-isotope measurement will be the first in this kinematic region. Using isotopes, we will be able to study the isospin dependence of the 2N-SRCs in inclusive scattering to complement the two-nucleon knockout measurements. This experiment will be the first measurement of the isospin dependence of 3N-SRC.

This is a high impact measurement testing the scaling assumptions made in the CLAS analysis of 3N-SRC, and making a factor of 2 improvement on both the direct experimental measurement and the extraction of information on three-nucleon correlations. The mapping of the x and Q^2 dependence from our proposed experiment will help in the optimization of already-proposed 12 GeV measurements on several few-body and heavy nuclei. It will also be very useful in determining the feasibility of similar measurements on ^3H and ^3He at 12 GeV.

-
- [1] L. L. Frankfurt and M. I. Strikman, Nucl. Phys. **B181**, 22 (1981).
 - [2] L. L. Frankfurt and M. I. Strikman, Phys. Rept. **160**, 235 (1988).
 - [3] C. C. degli Atti and S. Simula, Phys. Lett. B **325**, 276 (1994).
 - [4] L. L. Frankfurt, M. I. Strikman, D. B. Day, and M. Sargsian, Phys. Rev. C **48**, 2451 (1993).
 - [5] K. S. Egiyan et al. (CLAS), Phys. Rev. C **68**, 014313 (2003).
 - [6] K. S. Egiyan et al. (CLAS), Phys. Rev. Lett. **96**, 082501 (2006).
 - [7] W. Bertozzi, E. Piassetzky, J. Watson, S. Wood, et al., Jefferson Lab experiment E01-015.
 - [8] R. Shneor et al. (Jefferson Lab Hall A), Phys. Rev. Lett. **99**, 072501 (2007).
 - [9] K. Egiyan et al., cLAS-NOTE 2005-004, www1.jlab.org/ul/Physics/Hall-B/clas.
 - [10] M. M. Sargsian, private communication.
 - [11] E. Piassetzky, M. Sargsian, L. Frankfurt, M. Strikman, and J. W. Watson, Phys. Rev. Lett. **97**, 162504 (2006).
 - [12] J. L. S. Aclander et al., Phys. Lett. **B453**, 211 (1999).
 - [13] A. Tang et al., Phys. Rev. Lett. **90**, 042301 (2003).
 - [14] E. Piassetzky, private communication.
 - [15] R. Schiavilla, R. B. Wiringa, S. C. Pieper, and J. Carlson, Phys. Rev. Lett. **98**, 132501 (2007).
 - [16] S. C. Pieper and R. B. Wiringa, Ann. Rev. Nucl. Part. Sci. **51**, 53 (2001), nucl-th/0103005.
 - [17] B. Wiringa, private communication.
 - [18] G. Petratos, J. Gomez, R. Holt, R. D. Ransome, et al., Jefferson Lab proposal E06-12-118 (conditionally approved).
 - [19] T. Frick, H. Muther, A. Rios, A. Polls, and A. Ramos, Phys. Rev. **C71**, 014313 (2005).
 - [20] D. Meekins, private communication.

- [21] N. Fomin, Ph.D. thesis, University of Virginia (in preparation).
- [22] J. Arrington et al., Phys. Rev. Lett. **82**, 2056 (1999).
- [23] P. Solvignon, Ph.D. thesis, Temple University (2006).
- [24] J. Alcorn et al., Nucl. Inst. & Meth. **A522**, 294 (2004).
- [25] O. Benhar, D. day, and I. Sick (2006), nucl-ex/0603029.
- [26] Z. E. Meziani et al., Phys. Rev. Lett. **69**, 41 (1992).
- [27] J. Seely, Ph.D. thesis, Massachusetts Institute of Technology (2006).